Journal of Catalysis 256 (2008) 287–292

Contents lists available at ScienceDirect

Journal of Catalysis

www.elsevier.com/locate/jcat

Effect of coadsorbed water on the photodecomposition of acetone on $TiO_2(110)$

Michael A. Henderson

Interfacial Chemistry and Engineering Group, Pacific Northwest National Laboratory, P.O. Box 999, MS K8-87, Richland, WA 99352, USA

ARTICLE INFO

Article history:
Received 18 January 2008
Revised 18 March 2008
Accepted 21 March 2008
Available online 23 April 2008

Keywords:
Photocatalysis
TiO_2
Acetone
Water
TPD

ABSTRACT

The influence of coadsorbed water on the photodecomposition of acetone on TiO_2 was evaluated using temperature-programmed desorption (TPD) and the rutile $TiO_2(110)$ surface as a model photocatalyst. Of the two major influences ascribed to water in the heterogeneous photocatalysis literature (promotion through OH radical supply and inhibition due to site blocking), only the negative influence of water was observed. As long as the total water + acetone coverage was maintained well below the first-layer saturation coverage (1 ML), little inhibition of acetone photodecomposition was observed. However, as the total water + acetone coverage exceeded 1 ML, acetone was preferentially displaced from the first layer to physisorbed states by water, and the extent of acetone photodecomposition was attenuated. The immediate product of acetone photodecomposition was adsorbed acetate, which occupies twice as many surface sites per molecule as acetone. Because the acetate intermediate was more stable on the $TiO_2(110)$ surface than either water or acetone (as gauged by TPD), and because it had a lower photodecomposition rate than acetone, additional surface sites were not opened up during acetone photodecomposition to allow previously displaced acetone molecules to reenter the first layer.

1. Introduction

Water has the ability to act as either a poison or a promoter in photochemical reactions occurring on the surfaces of TiO_2 photocatalysts [1–24]. This seemingly contradictory behavior of water is commonly seen in the photooxidation reactions of organics. As a promoter, water is believed to supply the catalyst with the means of generating OH radicals that participate in the oxidation reactions. Two of the main mechanisms for OH• formation proposed in the literature involve hole-mediated oxidation of adsorbed hydroxyl anions and the reaction of water with O_2^- (formed by electron attachment to O_2), resulting in OH• through HO_2•. Water also is believed to promote halocarbon photooxidation reactions by enhancing the removal of Cl from the catalyst surface (in the form of HCl) [1]. In contrast, water also has been shown to act as a poison in organic photooxidation reactions. Water's inhibiting influence results from its stronger binding to TiO_2 surfaces compared with many organic species. Like most oxides, TiO_2 binds water strongly, particularly as dissociative fragments [25]. The interaction of water with TiO_2 tends to be stronger than the interactions of such organics as alkanes, alkenes, and aromatics, which lack the functional groups needed to form strong electrostatic interactions with surface cation sites. In contrast, such organics as alcohols and carboxylic acids tend to bind as strongly or more strongly to TiO_2 compared with water and may not be displaced by water. Strongly repulsive hydrophilic–hydrophobic interactions between coadsorbed water and organics will result in displacement of weakly bound organics from the catalyst surface, but segregation of more strongly bound organics into regions of high organic coverage. The interfacial boundaries between these hydrophilic and hydrophobic domains are regions of unusual activity and variability [26,27].

The opposing roles of water in organic photooxidation reactions on TiO_2 pose a considerable barrier to understanding the overall rates and mechanisms in photocatalysis. For example, although the first step in a gas-phase organic photooxidation process may be promoted by water, the oxidation steps of the resulting intermediates and products are inhibited. As the overall reaction progresses, more water is generated by oxidation, further complicating the reaction. The surface coverages of water, the various types of organics present, and molecular oxygen are in dynamic flux. Heterogeneity of the oxide surface also comes into play, because the local surface structure affects how these molecular components of the overall reaction compete and cooperate. Gaining true insight into the collective positive and/or negative influences of water on a typical organic photooxidation reaction is difficult. Understanding the influence of water (on the molecular and local scales) at the various stages of the oxidation process will provide information as to which interactions are important at the various points in the overall reaction process.

In this work, the influence of water on the photoconversion of acetone to acetate on the rutile $TiO_2(110)$ surface is examined using an ultra-high-vacuum (UHV) approach. Whereas UHV provides somewhat of an artificial environment for studying a photocat-

---

E-mail address: ma.henderson@pnl.gov.

0021-9517/$ – see front matter © 2008 Elsevier Inc. All rights reserved.
doi:10.1016/j.jcat.2008.03.020

alytic reaction in that it precludes the influence of a "solvent-like" environment of water at the surface, it has the advantage of providing a clearer view of molecular-level interactions than can be obtained under typical reaction conditions. In the case at hand, the formation of "free" OH• can be precluded, due to the absence of an aqueous phase. Under these conditions, the molecular-level interactions between water and the organic become the marquee influence on the photooxidation reaction. The (110) face of rutile TiO_2, which is the prototypical oxide surface and a major contributor to the surface area of nanocrystalline rutile, provides a well-characterized and well-understood environment [28] in which to evaluate the molecular-level influence of water on organic photooxidation.

Acetone photooxidation on TiO_2 has received considerable attention in the literature [10–16,18–20,22–24,29–38], with most studies using acetone to test new photocatalysts or new reactor concepts. Less work has been focused on the mechanistic details of the reaction. Using FTIR, El-Maazawi et al. [14] proposed several mechanistic pathways for the photooxidation of acetone on TiO_2, including a pathway involving dimerized acetone species and pathways that lead through surface intermediates such as carboxylates. Formate, acetate, acetaldehyde, and formic acid have been observed as surface intermediates in acetone photooxidation [34,35]. In addition, Attwood et al. [36] used EPR to identify a organoperoxy intermediate resulting from acetone photooxidation on TiO_2. This species was stable up to 150 K but decomposed above this temperature. Earlier work revealed that acetone photodecomposition on TiO_2(110) involved conversion of acetone to an acetone diolate species [$(CH_3)_2CO_2$] through a thermal reaction with oxygen, followed by photodecomposition of the diolate to adsorbed acetate (CH_3CO_2) and ejection of a methyl radical from the surface [39,40]. A similar process occurred for butanone photodecomposition on TiO_2(110), except that the ethyl group was preferentially ejected, leaving acetate on the surface [41].

Numerous groups have investigated the effect of water on the photooxidation of acetone on TiO_2. The conclusions from these studies vary considerably. For example, several groups have reported little or no enhancement of acetone photooxidation rates at low relative humidity (RH) but significant rate inhibition at higher RH [11–13,15,18–21]. The RH at which the rate was adversely influenced was generally around 15–20%. Based on isothermal adsorption studies, this inhibitory effect has been attributed to water's ability to block sites and displace adsorbed acetone from the surface [18–20,23]. For example, Kozlov et al. [23] reported that their TiO_2 photocatalyst surface was covered with 1 ML of water at 20 °C for RH $>$ 30%, and that this water coverage was sufficient to prevent acetone from interacting with photoexcited charges generated by UV absorption. Other groups have reported a slightly enhanced acetone photooxidation rate at low RH but significant inhibition at higher RH [23,24]. The low-RH enhancement is attributed to the ability of water to form surface OH^- groups, which in turn can be converted photochemically to OH•. At higher RH, water populates the surface and prevents acetone adsorption. Other groups have found no inhibition effect at all. Coronado et al. [22] observed a ∼50% decrease in the acetone uptake with increasing RH up to 28% (and not much change in the acetone adsorption behavior above this RH), but also noted that the acetone photooxidation rate increased by ∼50% as the RH was increased from 0 to 20% and remained fairly constant above 20% RH. Based on these data, these authors proposed that acetone uptake is not the rate-limiting factor in acetone photooxidation. Similarly, Chen et al. [10] observed a tripling in the acetone photooxidation rate with increasing mole fraction of H_2O in the reactant mixture, followed by a slight decline in the rate for mole fractions above 0.005 (∼15% RH). The increase was attributed to involvement of OH• and the decrease due to water site blocking; the former effect appeared to dominate the latter effect at higher RH, resulting in an overall enhancement. Other groups have reported that the acetone photooxidation rate can be enhanced by hydroxylation of the surface before the reaction [14,17]; again, this enhancement was attributed to the production of OH radicals.

Many conditions may come into play to explain these varying results. Temperature clearly plays a role in the influence of water on acetone photooxidation. Although increasing the reaction temperature appears to slightly inhibit the rate of acetone photooxidation under dry conditions [11,12], increased temperature (above room temperature) also tends to negate the inhibiting influence of water; for example, Vorontsov et al. [15] found inhibition of acetone photooxidation at 40 °C by water at a RH of ∼30%, and Chang et al. [16] found little or no effect of water vapor on the acetone photooxidation rate at 138 °C. Increasing the reaction temperature above RT shifted the water isotherm out toward higher RH levels. In fact, Vorontsov observed that with increasing reaction temperature, the RH level at which rate inhibition occurred continually increased, reflecting the decreased H_2O adsorptive capacity of TiO_2 as a function of increasing temperature. The form of the TiO_2 catalyst (e.g., anatase, rutile, a mixture) may be important, as may be the relative oxygen partial pressure or the presence of impurities that catalyze secondary reactions.

2. Experimental

The UHV chamber used in this study had a base pressure of 2×10^{-10} Torr. The TiO_2(110) crystal, with dimensions of $10 \times 10 \times 1.5$ mm, was obtained from First Reaction [42]. In this study, one monolayer (1 ML) is defined as the surface site density of five-coordinated Ti^{4+} cation sites on the ideal TiO_2(110) surface (5.2×10^{14} molecules/cm^2). The surface was cleaned by sputter-anneal cycles and deemed to be clean by analysis with secondary ion mass spectrometry (SIMS) and Auger electron spectroscopy (AES). Additional details on cleaning and sample preparation are available elsewhere [40]. After the initial cleaning, the crystal was deep blue, and its surface exhibited an oxygen vacancy population of about 0.07 ML as gauged by water TPD. Routine daily cleaning was done by annealing the crystal at 850 K for ∼10 min in UHV. These annealing treatments did not significantly affect the oxygen vacancy population.

Research-grade acetone and water were obtained from Aldrich and further purified using liquid nitrogen (LN2) freeze-pump-thaw cycles. Vapors from both liquids were exposed to the TiO_2(110) surface at 95 K. A calibrated pinhole directional doser enabled accurate dosing and prevented exposure to any surface (e.g., the sample holder) other than the crystal face. Oxygen gas was dosed by backfilling the chamber after passing the gas through a LN2-cooled trap. TPD experiments were performed at a heating rate of 2 K/s.

An Oriel 100-W Hg arc lamp was used for controlled UV irradiation. After being passed through a distilled water filter (to remove IR), the light was focused onto the tip of a single-strand, 0.6-mm-diameter fused silica fiberoptic cable directly coupled to vacuum by a UHV-compatible feedthrough. The use of a fiberoptic system provided light irradiation only to the crystal surface. A feedback system mounted on the lamp's housing maintained a constant photon flux during lamp operation. The photon flux emitted from the fiberoptic system before it entered the chamber was regularly checked using a photodiode detector. Calibration was obtained from the ratio of light intensity lost (because of fiber optic couplings) between the air side of the UHV fiberoptic feedthrough and the sample surface (measured before bakeout of the chamber). The UV component of the lamp's output was calibrated using a 400-nm cutoff filter. Photon exposures were started and ended using a mechanical shutter situated on the lamp's hous-

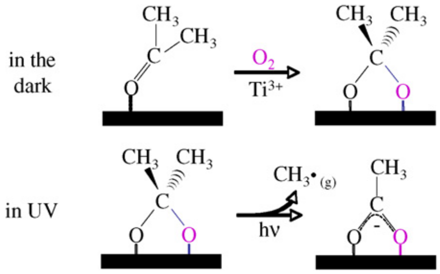

Fig. 1. Mechanistic scheme for the photodecomposition of acetone to acetate on the $TiO_2(110)$ surface.

ing. A typical flux of UV photons at the crystal was on the order of 1×10^{17} photons/cm^2. Irradiation of the $TiO_2(110)$ crystal at 95 K with this photon flux raised the crystal temperature to 105 K.

3. Results and discussion

Fig. 1 shows the proposed reaction scheme for the photodecomposition of acetone on the $TiO_2(110)$ surface [40]. This process essentially involves two steps. The first step, occurring without the direct influence of light, involves a thermal reaction between an adsorbed acetone molecule and an adsorbed oxygen species to form an acetone diolate. This reaction is facilitated by a charge transfer from Ti^{3+} sites (e.g., an oxygen vacancy) to O_2, which allows adsorption of the latter on the surface. In this sense, light participates in the first step by preparing electron trap sites (essentially Ti^{3+} sites) at which O_2 can chemisorb on the surface. In these experiments, the surface is artificially enhanced with Ti^{3+} sites in the form of oxygen vacancies [28]. The acetone diolate groups created in the dark decompose rapidly on irradiation with UV. Additional acetone photodecomposition occurs at a much slower rate. Whether acetone reacts directly with chemisorbed O_2, or whether O_2 is dissociatively adsorbed first and a resulting O fragment reacts with acetone, is unclear. The acetone diolate has been characterized with high-resolution electron energy loss spectroscopy (HREELS) and ^{18}O-labeling TPD studies [39]. Clearly, formation of the acetone diolate species involves rehybridization of the carbonyl portion of acetone based on HREELS results. Whereas acetone bound in the η^1 configuration (top left of Fig. 1) appears to be photoinactive on $TiO_2(110)$ under UHV conditions, the acetone diolate decomposes on exposure of the crystal to UV light. The decomposition process involves prompt rupture of one of the C–CH_3 bonds and ejection of the corresponding methyl radical into vacuum. The resulting acetate group is retained on the surface (in TPD to >550 K) and is considerably less susceptible to photodecomposition than the acetone diolate species. A consequence of acetate's stability is that the photoreaction is somewhat self-limiting under true catalytic conditions at room temperature, because the immediate product (acetate) is more strongly bound and less photoactive than the starting reactant acetone. This situation is in contrast to the hole-mediated decomposition of trimethyl acetate (TMA) [26,27,43,44], where the photofragments are not retained on the surface at room temperature. In the case of TMA, irradiation has the general effect of "clearing off" regions of organic from the surface. This two-step reaction process, shown in Fig. 1, appears to be the dominant pathway for photodecomposition of other organic carbonyls on the $TiO_2(110)$ surface [41].

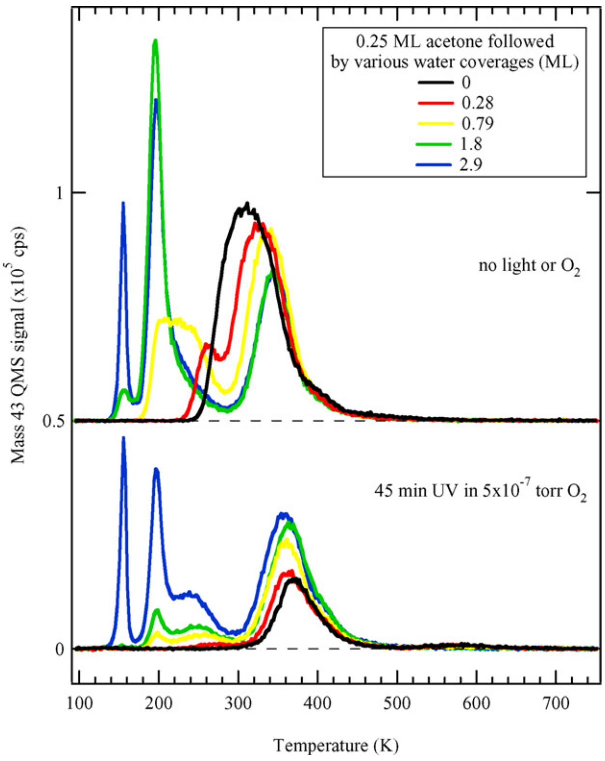

Fig. 2. Mass 43 TPD spectra from various coverages of water coadsorbed with 0.25 ML acetone on $TiO_2(110)$ at 95 K. The upper set (displaced vertically for clarity) is without photooxidation treatment and the lower set is after 45 min of UV exposure in 5×10^{-7} Torr O_2 at 105 K.

Although water is not a byproduct in the two-step acetone photodecomposition scheme shown in Fig. 1, it is a byproduct of the complete acetone photooxidation to CO_2. Water also is prevalent on oxide surfaces under most conditions. As such, the influence of coadsorbed water on the two-step acetone photodecomposition mechanism of Fig. 1 merits examination. Previous work has demonstrated that water and acetone compete for similar adsorption sites on the $TiO_2(110)$ surface, but water does not significantly affect the acetone diolate species once it is formed [45]; therefore, it is the competition between water and acetone for adsorption sites that is most likely to affect the photodecomposition process in step 1. The top panel of Fig. 2 illustrates this competition in the absence of light. Here a fixed coverage of acetone (0.25 ML) was adsorbed at 95 K, followed by various coverages of water (also at 95 K). The surface was then heated in the TPD experiment. In the absence of water, 0.25 ML acetone desorbed from $TiO_2(110)$ in a broad peak centered at about 300 K (black trace). As water was added to the surface, a "dip" developed in the acetone TPD trace at about 270 K (red trace corresponding to 0.28 ML of water), with some acetone TPD intensity shifting to lower temperatures than were observed on the clean surface. The "dip" corresponds to the peak temperature for thermal desorption of first layer water from the $TiO_2(110)$ surface [45,46]. As more water was added, the dip in the acetone TPD spectrum widened, and proportionally more acetone TPD intensity shifted to lower temperature (yellow, green, and blue traces). The amount of acetone displaced in TPD to lower temperature by coadsorbed water appeared to saturate for water coverage >1 ML (blue and green traces). The sharp acetone TPD states at ∼160 and 200 K are assigned to acetone ice and acetone hydrogen-bonded to dangling OH bonds of adsorbed water, respectively [45]. Based on these data, whether the displacement process occurred on adsorption of water at 95 K or during TPD is unclear, but a significant portion of the displacement clearly occurred before the onset of the acetone ice peak (∼130 K).

Acetone and water bind to the $TiO_2(110)$ surface at the same sites [39,46], the 5-coordinate Ti^{4+} cations. Acetone is displaced by water, because water adapts more readily than acetone to intermolecular repulsions in the first layer [45]. Despite the fact that an isolate acetone molecule binds more strongly to the $TiO_2(110)$ surface than an isolated water molecule, dipole–dipole repulsions between acetone molecules significantly reduce acetone's binding energy; as a result, acetone is more readily displaced from the first layer. However, even under conditions of excess water, some acetone is retained on the surface at desorption temperatures above room temperature. This occurs either because isolate acetone molecules (with only water as nearest neighbors) are stable on the surface or because water desorption during the TPD experiment (which begins at ∼200 K and peaks at 270 K) eventually alleviates surface adlayer stress, allowing access of some physisorbed acetone to the first layer.

It has been shown previously that the rate of acetone photodecomposition on $TiO_2(110)$ is coverage-dependent, with the rate for a saturated monolayer is roughly an order of magnitude lower than for a 0.25-ML coverage [40]. This effect is attributed to O_2's inability to penetrate an acetone-saturated surface. The impact of water coadsorption on the photodecomposition of acetone is explored in the TPD data of the lower panel of Fig. 2. In these data, a set coverage of acetone (0.25 ML) was exposed to various coverages of water at 95 K and then irradiated with UV light (for 45 min) in 5×10^{-7} Torr O_2 at 105 K. The data in the top panel of Fig. 2 provide a direct comparison for the nonirradiated coadsorbed system at each coverage combination. The amount of photodecomposed acetone in each case can be determined through comparison with the peak area of the TPD traces for the nonirradiated conditions. In the absence of water (black trace in the lower portion of Fig. 2), roughly 75% of the starting 0.25 ML acetone coverage was photodecomposed during the 45-min irradiation period. This result is consistent with previous findings [40]. Coadsorption of 0.28 ML of water (red curve) had only a slight effect on acetone photodecomposition. In this case, the total coverage of acetone and water was ∼0.53 ML; thus, likely no displacement of acetone from the first layer by water occurred, and sufficient sites were available to allow O_2 to participate in the reaction. A nuance of this conclusion is that the number of sites required for acetone photodecomposition should be double the number required to bind acetone in first place, because both the acetone diolate intermediate and the product acetate require two sites per species, whereas acetone requires only one site. Whether or not the acetone diolate or acetate species once formed can displace coadsorbed water (or acetone) is unknown. At a combined acetone and water coverage of ∼1 ML (0.25 and 0.79 ML, respectively), the total number of sites required to complete the two-step reaction and still accommodate all of the adsorbed water in the first layer would be ∼1.25 ML, which is not possible. The yellow trace in the bottom panel of Fig. 2 indicates that a significantly greater amount of acetone remained unreacted on the surface compared with the clean and 0.28-ML water cases. The inhibiting influence of water continued, with coadsorption of 1.8 ML (green trace) and 2.9 ML (blue trace) of water. The 2.9-ML coverage is nearly sufficient to completely prevent any photodecomposition of the preadsorbed 0.25-ML coverage of acetone. These TPD data clearly demonstrate the inhibiting effect of coadsorbed water on the photodecomposition of acetone on $TiO_2(110)$ under UHV conditions.

Fig. 3 further illustrates the affect of water on acetone photodecomposition from the standpoint of the amount of acetate product formed (see Fig. 1). Acetate thermally decomposes on $TiO_2(110)$ at ∼600–700 K [47], predominately through a unimolecular process that yields ketene (CH_2CO) and OH [40]. The latter rapidly disproportionates to form water. Fig. 3 shows mass 42 TPD traces for the same data as shown in the lower panel of Fig. 2. As shown by comparing these traces with those shown in Fig. 2, the desorption features at temperatures below 450 K are from acetone, which has a small QMS cracking contribution at mass 42. (The dashed trace is from the mass 42 signal arising from TPD of 0.25 ML of acetone on the clean surface without light.) The desorption features at temperatures above 450 K are due to ketene based on the ratios of the mass 42 to 28 to 14 signals (not shown). No mass 42 signal was observed above 450 K in the absence of photochemistry (dashed trace). The amount of ketene produced was about the same for acetone alone and for acetone coadsorbed with 0.28 ML of water (black and red traces, respectively). An approximate 20% decrease in ketene formation was observed with a water coadsorption coverage of 0.79 ML. The amount of ketene formed continued to decrease as more water was added to the surface before UV irradiation. No other photoreaction products were observed, suggesting that under UHV conditions, coadsorbed water did not steer the acetone photodecomposition mechanism in a new direction.

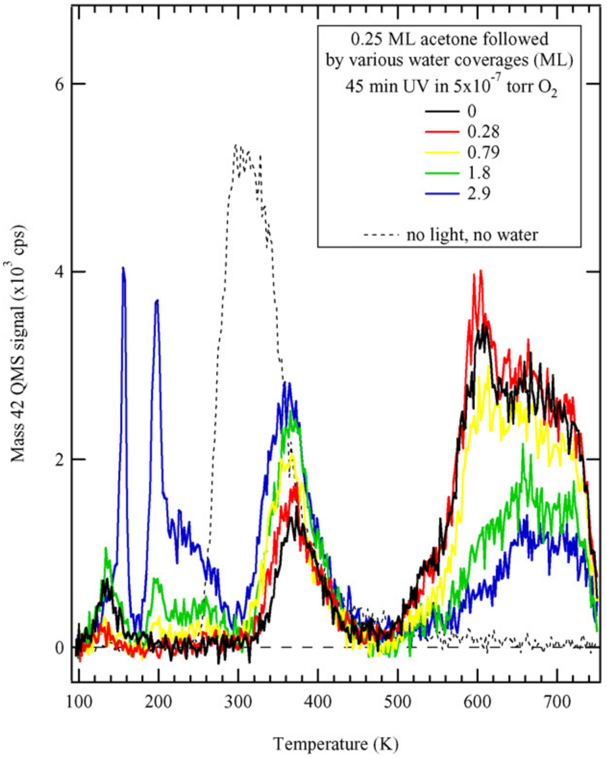

Fig. 3. Mass 42 TPD spectra from the acetone photooxidation data shown in the lower portion of Fig. 2. The dashed trace is the mass 42 signal from TPD of 0.25 ML acetone on the clean $TiO_2(110)$ surface.

The amounts of depleted acetone and generated acetate are shown in Fig. 4. The acetone is shown as the fraction of acetone depleted relative to the starting coverage of 0.25 ML (the axis on the left), and the acetate is expressed as the mass 42 TPD peak area from ketene (the axis on the right). The latter is scaled to fit over the former. Both metrics show roughly the same effect. Low water coverage has only a slight influence on acetone photodecomposition, whereas higher coverage exerts a systematic attenuating influence on acetone photodecomposition. No apparent promotion of acetone photodecomposition occurs under these conditions.

Interpreting the adverse affect of water on the acetone photodecomposition yield appears to be fairly straightforward. Even at 105 K, a large exposure of water appears to displace acetone from the first layer into physisorbed states. The photodecomposition efficiency of physisorbed acetone, either through a direct excitation process (such as is seen in the gas phase) or through a charge transfer from the surface, is considerably less efficient than that of the reaction scheme shown in Fig. 1. Under the conditions of these experiments, the photodecomposition of acetone in the first layer does not open up surface sites for similar processing of physisorbed acetone molecules, because the reaction product, acetate, is bound more strongly than water and blocks twice as many sites as needed for acetone. Acetate also appears to be photolytically more stable on the $TiO_2(110)$ surface than the reactant acetone. Although the data presented here assume only one starting cov-

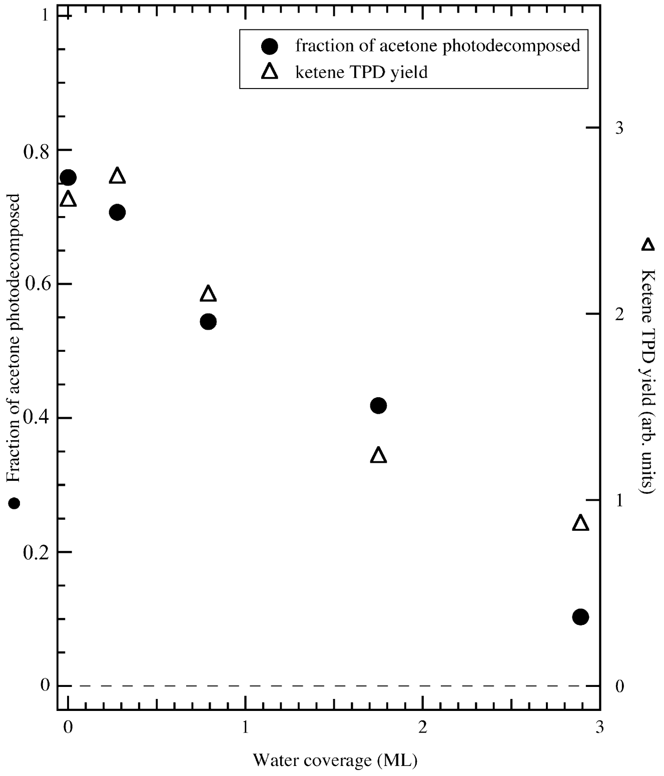

Fig. 4. Fraction of acetone photodecomposed (left axis) and yield of ketene from thermal decomposition of photogenerated acetate (right axis) both as a function of water coadsorption coverage on the $TiO_2(110)$ surface. Data is taken from the TPD traces shown in Figs. 2 and 3. The scale of the right axis is arbitrarily set so the two sets of data overlay each other.

erage for acetone, interpretation of the data suggests that higher acetone coverage will cause inhibition at lower coadsorption coverages of water (and vice versa for lower coverages of acetone). The key factor in the inhibition of acetone photodecomposition by water appears to occur at the molecular level, involving water's ability to compress acetone into local regions of high coverage that destabilize chemisorbed acetone, causing its displacement from the first layer (even at 105 K).

4. Conclusion

These findings demonstrate that coadsorbed water has an inhibiting influence on the photodecomposition of acetone on the $TiO_2(110)$ surface under UHV conditions. At low water and acetone coverage, the inhibiting influence of water was not seen because sufficient surface sites were available to accommodate reaction intermediates and products (which occupy more sites per species than acetone) and to allow gas-phase O_2 access to the surface; however, the rate of acetone photodecomposition was inhibited as the total acetone plus water coverage approached first-layer saturation. Virtually no acetone photodecomposition was detected with $\sim$3 ML of coadsorbed water. Two factors contribute to this inhibition: the displacement of acetone from the first layer to the physisorbed layer by coadsorbed water, and the blocking of O_2's access to the surface by high collective coverage of water and acetone. Because the dynamics of the water layers used in these UHV studies are "frozen out" at the irradiation temperature used (105 K), water coverage in excess of 1 ML on TiO_2 surfaces can displace most of the preadsorbed acetone and prevent O_2 adsorption. Water's inhibitory effect should be less severe for similar water coverage under typical applied conditions (at room temperature in solution or humid atmospheres) than is found under UHV conditions because dynamics in the water film will allow access of some acetone and oxygen to the surface.

Acknowledgments

This work was supported by the U.S. Department of Energy, Office of Basic Energy Sciences, Division of Chemical Sciences. Pacific Northwest National Laboratory is a multiprogram national laboratory operated for the U.S. Department of Energy by the Battelle Memorial Institute under contract DEAC06-76RLO1830. The research reported here was performed in the William R. Wiley Environmental Molecular Science Laboratory, a Department of Energy user facility funded by the Office of Biological and Environmental Research.

References

[1] X. Fu, W.A. Zeltner, M.A. Anderson, Stud. Surf. Sci. Catal. 103 (1996) 445–461.
[2] C. Belver, M.J. Lopez-Munoz, J.M. Coronado, J. Soria, Appl. Catal. B Environ. 46 (2003) 497–509.
[3] C. Hagglund, B. Kasemo, L. Osterlund, J. Phys. Chem. B 109 (2005) 10886–10895.
[4] A. Yamakata, T.A. Ishibashi, J. Onishi, J. Phys. Chem. B 107 (2003) 9820–9823.
[5] M.C. Blount, J.L. Falconer, Appl. Catal. B Environ. 39 (2002) 39–50.
[6] D.R. Park, J.L. Zhang, K. Ikeue, H. Yamashita, M. Anpo, J. Catal. 185 (1999) 114–119.
[7] D.S. Muggli, M.J. Backes, J. Catal. 209 (2002) 105–113.
[8] M. Kang, J. Mol. Catal. A Chem. 197 (2003) 173–183.
[9] M.L. Sauer, D.F. Ollis, J. Catal. 158 (1996) 570–582.
[10] S.F. Chen, X.L. Cheng, Y.W. Tao, M.Y. Zhao, J. Chem. Technol. Biotechnol. 73 (1998) 264–268.
[11] S.B. Kim, H.T. Hwang, S.C. Hong, Chemosphere 48 (2002) 437–444.
[12] S.B. Kim, S.C. Hong, Appl. Catal. B Environ. 35 (2002) 305–315.
[13] W. Choi, J.Y. Ko, H. Park, J.S. Chung, Appl. Catal. B Environ. 31 (2001) 209–220.
[14] M. El-Maazawi, A.N. Finken, A.B. Nair, V.H. Grassian, J. Catal. 191 (2000) 138–146.
[15] A.V. Vorontsov, E.N. Kurkin, E.N. Savinov, J. Catal. 186 (1999) 318–324.
[16] C.-P. Chang, J.-N. Chen, M.-C. Lu, J. Environ. Sci. Health, A Toxic/Hazard. Subst. Environ. Eng. A 38 (2003) 1131–1143.
[17] J. Yu, H. Yu, B. Cheng, M. Zhou, X. Zhao, J. Mol. Catal. A Chem. 253 (2006) 112–118.
[18] C. Raillard, V. Hequet, P. Le Cloirec, J. Legrand, J. Photochem. Photobiol. A Chem. 163 (2004) 425–431.
[19] M.L. Sauer, D.F. Ollis, J. Catal. 149 (1994) 81–91.
[20] J. Peral, D.F. Ollis, J. Catal. 136 (1992) 554–565.
[21] G.B. Raupp, C.T. Junio, Appl. Surf. Sci. 72 (1993) 321–327.
[22] J.M. Coronado, M.E. Zorn, I. Tejedor-Tejedor, M.A. Anderson, Appl. Catal. B Environ. 43 (2003) 329–344.
[23] D.V. Kozlov, A.A. Panchenko, D.V. Bavykin, E.N. Savinov, P.G. Smirniotis, Russ. Chem. Bull. 52 (2003) 1100–1105.
[24] Y. Ku, K.Y. Tseng, W.Y. Wang, Water Air Soil Pollut. 168 (2005) 313–323.
[25] M.A. Henderson, Surf. Sci. Reports 46 (2002) 1–308.
[26] M.A. Henderson, J.M. White, H. Uetsuka, H. Onishi, J. Catal. 238 (2006) 153–164.
[27] H. Uetsuka, H. Onishi, M.A. Henderson, J.M. White, J. Phys. Chem. B 108 (2004) 10621–10624.
[28] U. Diebold, Surf. Sci. Reports 48 (2003) 53.
[29] J. Lin, J.C. Yu, D. Lo, S.K. Lam, J. Catal. 183 (1999) 368–372.
[30] A. Mattsson, M. Leideborg, K. Larsson, G. Westin, L. Osterlund, J. Phys. Chem. B 110 (2006) 1210–1220.
[31] Y. Umemura, E. Shinohara, A. Koura, T. Nishioka, T. Sasaki, Langmuir 22 (2006) 3870–3877.
[32] A.V. Vorontsov, A.A. Altynnikov, E.N. Savinov, E.N. Kurkin, J. Photochem. Photobiol. A Chem. 144 (2001) 193–196.
[33] M.E. Zorn, D.T. Tompkins, W.A. Zeltner, M.A. Anderson, Appl. Catal. B Environ. 23 (1999) 1–8.
[34] W. Xu, D. Raftery, J. Catal. 204 (2001) 110–117.
[35] J.M. Coronado, S. Kataoka, I. Tejedor-Tejedor, M.A. Anderson, J. Catal. 219 (2003) 219–230.
[36] A.L. Attwood, J.L. Edwards, C.C. Rowlands, D.M. Murphy, J. Phys. Chem. A 107 (2003) 1779–1782.
[37] C. Lv, X.J. Wang, G. Agalya, M. Koyama, M. Kubo, A. Miyamoto, Appl. Surf. Sci. 244 (2005) 541–545.
[38] C.M. Visinescu, R. Sanjines, F. Levy, V.I. Parvulescu, Appl. Catal. B Environ. 60 (2005) 155–162.
[39] M.A. Henderson, J. Phys. Chem. B 108 (2004) 18932–18941.
[40] M.A. Henderson, J. Phys. Chem. B 109 (2005) 12062–12070.

[41] M.A. Henderson, Surf. Sci. (2008), in press.
[42] This company is no longer in operation.
[43] M.A. Henderson, J.M. White, H. Uetsuka, H. Onishi, J. Am. Chem. Soc. 125 (2003) 14974–14975.
[44] J.M. White, M.A. Henderson, J. Phys. Chem. B 109 (2005) 12417–12430.
[45] M.A. Henderson, Langmuir 21 (2005) 3443–3450.
[46] M.A. Henderson, Surf. Sci. 355 (1996) 151–166.
[47] H. Idriss, P. Legare, G. Maire, Surf. Sci. 515 (2002) 413–420.